Applicability of power law for describing the rheology of soils of different origins and characteristics

Sueng Won Jeong, Serge Leroueil, and Jacques Locat

Abstract: The rate-dependent rheological behaviour of soils of different origins and characteristics was studied and the applicability of the power law model was examined. The studied soils were divided into three groups: (*i*) low-activity soils, (*ii*) high-activity soils, and (*iii*) silt-rich soils. The results show that the power law applies to all these soils and is representative of soil behaviour in a strain rate range corresponding to debris flows, which is generally not the case with the Bingham model. For low-activity clays, the power law index, *n*, is typically equal to 0.12 and seems to increase with the plasticity index; it is larger (i.e., in the range of 0.2–0.6) for silt-rich soils. Comparison of *n* values for tests performed on intact and remoulded low-activity clay specimens indicates that the power law index is possibly strain-rate dependent.

Key words: rheological behaviour, strain-rate effect, power law index, low- and high-activity clays, silt-rich and coarser soils.

Résumé : Le comportement rhéologique dépendant des taux a été étudié pour des sols ayant des origines et caractéristiques différentes, et l'applicabilité du modèle de la loi de puissance a été examinée. Les sols étudiés étaient divisés en trois groupes: (*i*) sols avec faible activité, (*ii*) sols avec activité élevée, et (*iii*) sols riches en silt. Les résultats montrent que la loi de puissance s'applique pour tous ces sols et est représentative du comportement pour des taux de déformation correspondants à des écoulements de débris, ce qui n'est généralement pas le cas avec le modèle de Bingham. Pour les argiles à faible activité, l'indice n de la loi de puissance est typiquement égal à 0,12 et semble augmenter avec l'indice de plasticité; n est plus élevé, variant de 0,2 à 0,6, pour des sols riches en silt. Des comparaisons entre les valeurs de n obtenues d'essais effectués sur des échantillons intacts et remaniés d'argile à faible activité indiquent que l'indice de la loi de puissance est possiblement dépendant du taux de déformation.

Mots-clés : comportement rhéologique, effet du taux de déformation, indice de la loi de puissance, argiles à activité faible et élevée, sols grossiers riches en silt.

[Traduit par la Rédaction]

Introduction

The knowledge of the rheological behaviour of remoulded soils is of paramount importance for understanding and analyzing mud and debris flows. In particular, it allows the determination of the velocity and run-out distance of debris, and thus helps in assessing the risk associated with these soil movements. Several rheological models have been proposed to describe the relationship between mobilized shear stress and shear strain rate. The most commonly used is the Bingham law (Imran et al. 2001), but other rheological models have also been proposed, including Herschel–Bulkley, Casson, power law, and the so-called bi-linear model (Locat and Demers 1988; Coussot 1997; Locat 1997). For the purpose of the present paper, only the Bingham and power law models are considered. They can be written as follows:

$$[1] \qquad \tau = \tau_c + \eta_h \gamma \qquad \text{(Bingham)}$$

$$[2] \qquad \tau = \eta \gamma^n \qquad \text{(power law)}$$

where τ is the shear stress (in Pa), τ_c is the yield stress (in Pa), and γ is the shear strain rate (in s^{-1}). It is worth insisting that γ is used here as strain rate and not as strain as in classical soil mechanics. In eq. [1], η_h is the plastic viscosity (in Pa·s). In eq. [2], the exponent n is the dimensionless power law index. For a n of 1, the power law model reduces to a Newtonian fluid model.

The parameters of eq. [1] are generally defined from laboratory viscometer tests for strain rates larger than about 20 s^{-1}. However, strain rates observed in debris flows are generally smaller than this value. Takahashi (1981) indicates that the observed velocities of debris flows are generally between about 0.5 and 20 m/s. Similar results were obtained by Lorenzini and Mazza (2004) and Ochiai et al. (2004). When typical strain rate (γ = du/dy) values are estimated from typical flow velocity (u) and flow depth (y) values, average strain rates encountered in the field typically range between 0.1 and 20 s^{-1} for debris flows (O'Brien and Julien

Received 17 September 2007. Accepted 2 March 2009. Published on the NRC Research Press Web site at cgj.nrc.ca on 19 August 2009.

S.W. Jeong[1] and S. Leroueil. Department of Civil Engineering, Laval University, Pavillion Adrien-Pouliot, local 2906, Québec City, QC G1K 7P4, Canada.
J. Locat. Department of Geology and Engineering Geology, Laval University, Pavillion Adrien-Pouliot, local 2906, Québec City, QC G1K 7P4, Canada.

[1]Corresponding author (e-mail: sueng-won.jeong.1@ulaval.ca).

Table 1. Physico-chemical identification of studied soils.

Sample	Water content, w_n (%)	Liquid limit, w_L (%)	Plastic limit, w_p (%)	Plasticity index, I_p (%)	Specific area, SS, (m^2/g)	Salinity, S (g/L)	Clay fraction, CF (%)	Activity, A_c*	Cation exchange capacity, CEC (meq/100 g)
Group 1									
Beaufort Sea	34.6	52	26	26	57	20	30	0.9	—
Cambridge Fjord	76	64	31	33	38	33	40	0.8	—
Hudson Apron	58.6	59.8	25.6	34.2	50–90	30	37–60	0.7	7–12
Jonquière	—	51.3	22.3	29.2	63–67	0.1	58–61	0.5	7–10
SAG 86 (Saguenay)	64	59	26	33	28	27.5	62	0.5	—
SAG 87 (Saguenay)	78	70	29	41	63	23.5	85	0.5	—
Pointe-du-Fort (Saguenay)	—	69.4	27.1	42.3	—	30	45	0.9	—
Adriatic Sea	75.7	65.6	36.1	29.5	15–90	30	9–27	1.1	6–12
Mediterranean Sea	67.5	62.8	24.4	38.4	—	28.97	52	0.7	—
St-Alban	45.0	33.1	16.1	16.9	40.1	0.85	38	0.4	—
Group 2									
Black Sea T1	177.7	121	43.7	77.3	—	23	59	1.3	—
Black Sea T2	214.5	183	55.8	127.2	—	22.5	40	3.2	29.3
Bentonite	—	353.4	53.9	299.5	—	0	77	3.9	—
	—	140.5	51.3	89.2	—	30	77	1.2	—
Group 3									
Iron tailing	—	22.3 (TU)	18.5	3.7	—	—	≤22	—	—
	—	22.9 (TF)	16.7	6.2	—	—	≤22	—	—

Note: TF, iron tailing flocculated; TU, iron tailing unflocculated.
*Activity $A_c = I_p$/CF.

1988; Phillips and Davies 1991; Major and Pierson 1992; Iverson 1997; Parsons et al. 2001). Moreover, linear τ–γ representations, such as the one used to define the parameters of the Bingham law, do not allow observation of behaviour at small strain rates. It is thus interesting to consider representations of the logarithm of strain rate that amplify behaviour at small strain rates. The power law (eq. [2]) thus appears interesting and its applicability to a variety of soils is examined in this paper.

Equation [2] describing the power law can also be written as follows:

$$[3] \qquad \log(\tau) = n\log(\gamma) + B$$

where, as compared with eq. [2], n is the power law index and B is a soil-dependent parameter. Equation [2] can also be written as follows, with τ normalized with respect to the reference shear stress τ_o at a reference shear strain rate γ_o:

$$[4] \qquad \log\left(\frac{\tau}{\tau_o}\right) = n\log\left(\frac{\gamma}{\gamma_o}\right)$$

Note that τ_o is not a yield stress, but the shear stress at an arbitrary value of γ_o. In addition to n, knowledge of τ_o at the reference shear rate γ_o is essential to obtain the complete rheological behaviour of the soil.

Jeong (2006) studied the rheological behaviour of about 12 soils of different origins with different grain-size distributions and mineralogies. The results thus allow the examination of the applicability of the power law and the evaluation of the corresponding parameters for a variety of materials. In addition, as it has been observed that the power law describes well the viscosity of intact clays (Leroueil 1996, 2006), a comparison of the viscous behaviour of intact and remoulded clayey soils can be made. The paper first presents the soils considered in this study and test methodology; the rheological behaviour of the soils, divided into three groups, is then presented; and a discussion and a conclusion follow.

Considered soils and test methodology

Soils considered

Over 12 soils with different mineralogies and grain-size distributions were used to determine their rheological characteristics. They are of different origins, but are composed mostly of clay and fine silt-sized particles. From the well-known Casagrande's plasticity chart and activity, the samples have been divided into three groups. Details on the physico-chemical properties of the studied soils are also given in Table 1.

Group 1 consists of natural inorganic clays of medium to high plasticity, which are described here as low-activity clays. The Jonquière clay, known as leached postglacial marine clay from Eastern Canada (Perret et al. 1996), is seen as a typical example of this group. The other clayey soils of the group of low-activity clays are clays from the Adriatic Sea, Beaufort Sea (northwestern Canada), Cambridge Fjord (Baffin Island, Canada), Hudson Apron (Offshore New York), Pointe-du-Fort (Upper Saguenay Fjord, Quebec), Mediterranean Sea, Jonquière (Quebec), and St-Alban

Fig. 1. Shear stress (τ, in Pa) and shear strain rate (γ, in s^{-1}) relationships at a given salinity (S = 1.0 g/L) but at different liquidity indices for the Jonquière clay: (*a*) τ versus γ, (*b*) log(τ) versus log(γ), and (*c*) normalized log(τ / τ_o) versus log(γ / γ_o), where τ_o and γ_o are reference shear stress and shear strain rate, respectively, when γ_o is taken to be 1 s^{-1}.

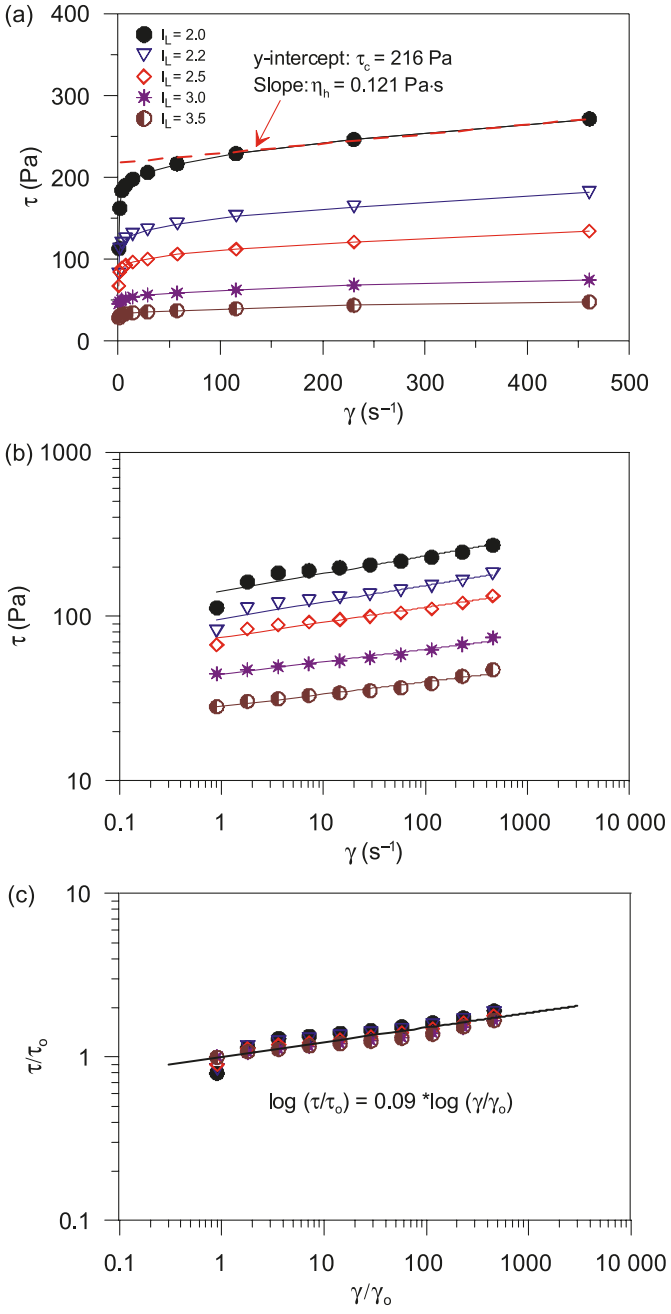

(Quebec). These materials have liquid limit (w_L) and plasticity index (I_P) values in the ranges of 35% to 75% and 15% and 50%, respectively; their activities are smaller than 1.15.

Group 2 consists of highly plastic clays containing montmorillonite or smectite and having high swelling capacity; they are described here as high-activity clays. The two soils from this group are natural clay from the Black Sea area and commercial bentonite from Wyoming. The Black Sea clays have a high content of smectite. The bentonite, supplied by

Fig. 2. Shear stress (τ, in Pa) and shear strain rate (γ, in s^{-1}) relationships in Jonquière clays with a given liquidity index (I_L = 2.5) and different salinities: (*a*) τ versus γ, and (*b*) normalized log(τ / τ_o) versus log(γ / γ_o), where τ_o and γ_o are reference shear stress and shear strain rate, respectively, when γ_o is taken to be 1 s^{-1}.

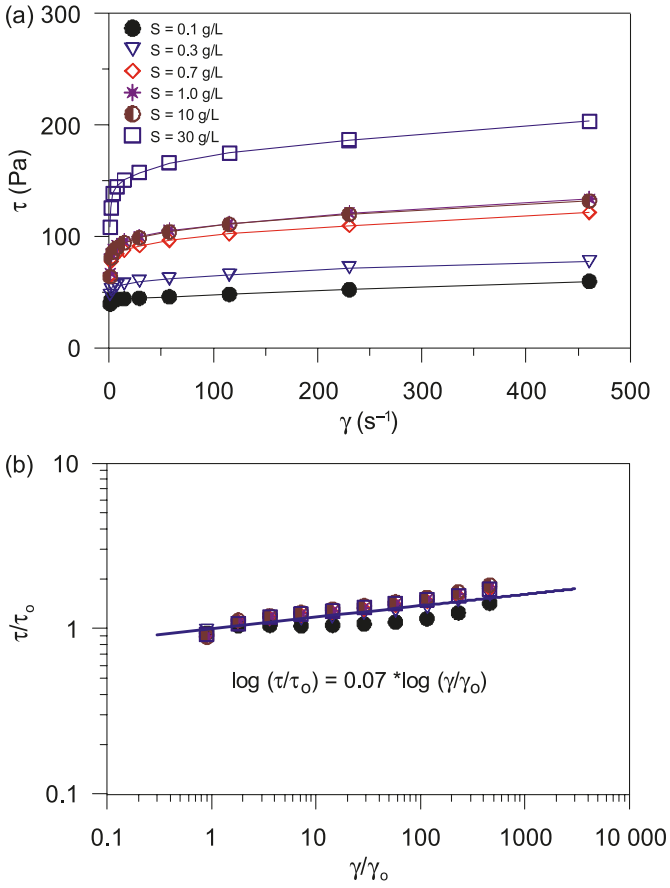

Black Hills Bentonite, LLC (Wyoming, USA), is highly plastic and swells readily in water to form thixotropic gel. For the purpose of this study, the bentonite powder was immersed in fresh or salt water and was allowed to freely swell for 24 h after dispersion; no change was observed when the soil was left for an additional 6 days. Soils of group 2 have liquid limits and plasticity indices in the 100% to 360% and 80% to 300% ranges and their activities are larger than 1.15.

Group 3 consists of iron ore tailings that essentially contain silt-sized particles with a small amount of clay (the fine sand fraction was removed for testing to respect the operational capacity of the rheometer). Two types of tailings, unflocculated and flocculated, were considered. Flocculation was achieved by adding a small amount of organic polymer. The samples were stored under tailings pond water (so there was no change in pore-water chemistry) in a suitable container for 24 h and were then air-dried. In this group, plasticity index (I_P) values are extremely small, 3.7% and 6.2% for the unflocculated and flocculated tailing samples, respectively. They are classified as inorganic clayey silts of low plasticity. Activities were between 0 and 0.3.

The study also includes tests performed by Malet et al. (2003). The strain rate effect was examined using different apparatuses for the two different soil fraction geometries: a

Fig. 3. Normalized flow curves ($\log(\tau / \tau_o)$ versus $\log(\gamma / \gamma_o)$) obtained on low-activity clays of different origins with a reference shear strain rate, γ_o, of 1 s^{-1}.

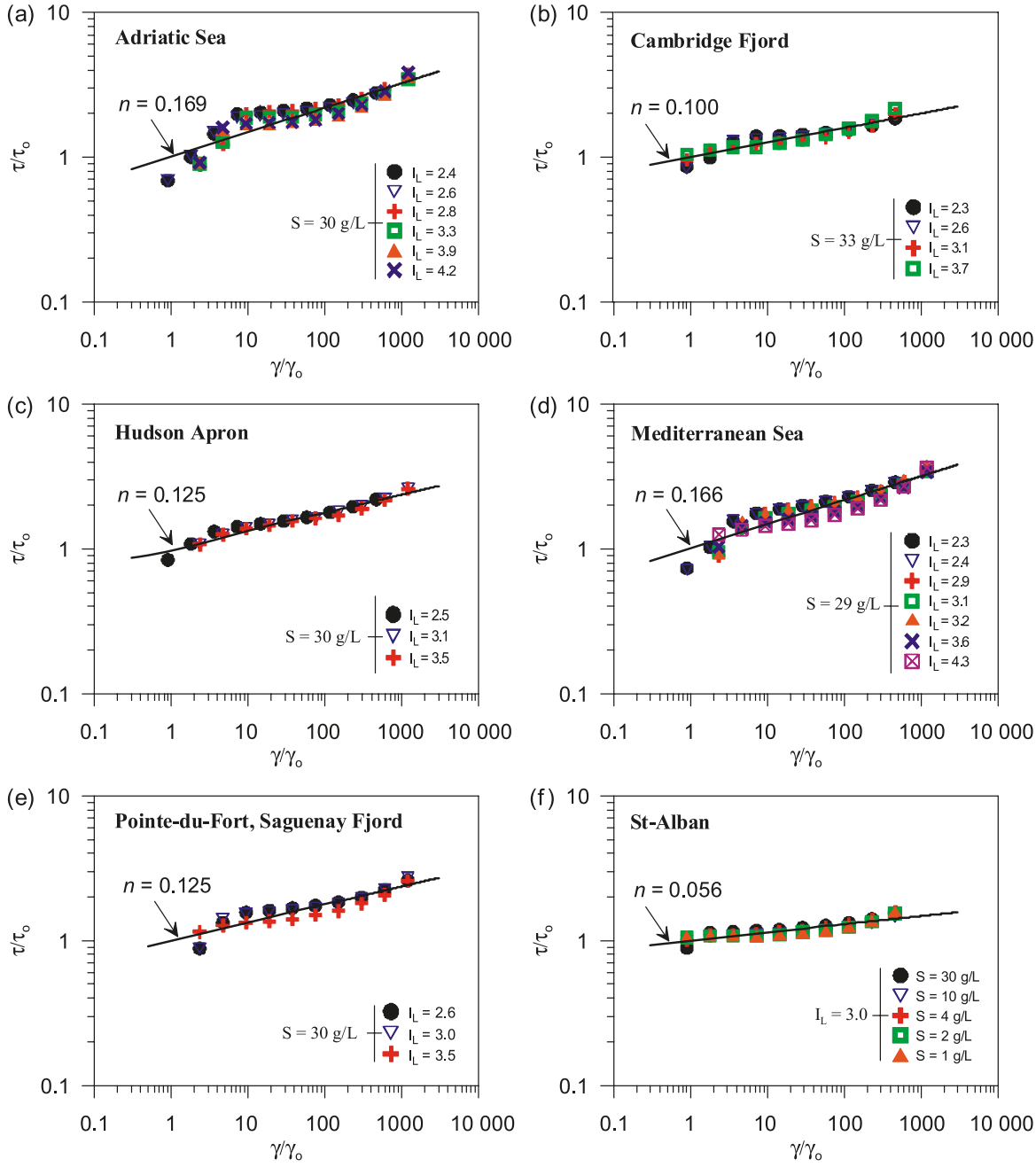

coaxial (CO) viscometer measured strain effect on the <0.075 mm soil fraction and a parallel-plate (PP) rheometer measured the same on the <0.4 mm soil fraction. The examined materials were taken from the South French Alps in the Barcelonnette Basin (Alpes-de-Haute Provence, France) from earthflows (La Valette; Poche) and debris-flow torrents (Faucon; Riou-Bourdoux). From the grain-size distributions shown by Malet et al. (2003), the clay content in the <0.075 mm soil fraction would not be so small, and the materials are rather clayey silts that are similar to the materials of group 3. As for the <0.4 mm fractions, they are coarser and, as they were studied using different equipment, they are not considered in the present study.

Test methodology

The rheological analyses of the sediments listed in Table 1 were carried out using a Rotovisco RV-12 coaxial cylinder (CO) viscometer. The procedure is described in detail by Locat and Demers (1988). Three types of tests were performed: (*i*) constant shear rate, (*ii*) dynamic response, and (*iii*) hysteresis measurements. Details on these tests are given by Jeong (2006). Malet et al. (2003) used the same

Table 2. Normalized flow properties obtained on remoulded soils of different origins.

Group 1: low-activity soils						
		Bingham model		Normalized flow curve		
Liquidity index, I_L	Salinity, S (g/L)	Shear stress, τ_c (Pa)	Viscosity, η_h (Pa·s)	Reference shear stress, τ_o (Pa)	Power law index, n	Coefficient of determination, r^2
Adriatic Sea						
2.4	30	157.9	0.104	73.7	0.188	0.804
2.6	30	126.3	0.087	58.9	0.179	0.807
2.8	30	81.3	0.049	37.5	0.18	0.848
3.3	30	62.9	0.042	32.5	0.164	0.852
3.9	30	32.5	0.028	18.4	0.131	0.828
4.2	30	23.5	0.022	13.0	0.165	0.838
Mediterranean Sea						
2.3	29	141.8	0.112	66.8	0.186	0.867
2.4	29	133.5	0.103	63.1	0.185	0.856
2.9	29	57.3	0.029	26.2	0.173	0.905
3.1	29	48.2	0.028	23.7	0.163	0.927
3.2	29	39.5	0.023	18.1	0.176	0.898
3.6	29	26.6	0.019	14.3	0.153	0.928
4.3	29	13.2	0.012	7.7	0.151	0.893
Beaufort Sea						
2.4	30	219.2	0.145	103.4	0.181	0.871
2.8	30	122	0.091	71.8	0.135	0.943
3.2	30	75.8	0.063	44.9	0.138	0.904
Cambridge Fjord						
2.3	33	120.5	0.074	83.8	0.102	0.856
2.6	33	75	0.061	52.9	0.103	0.874
3.1	33	33.3	0.036	25.2	0.095	0.924
3.7	33	17.5	0.021	12.7	0.111	0.907
Hudson Apron						
1.9	30	310.4	0.364	187.6	0.148	0.878
2.5	30	127.3	0.088	76.3	0.130	0.926
3.1	30	71.5	0.028	40.1	0.126	0.976
3.5	30	43.9	0.02	26.1	0.122	0.960
Saguenay Fjord						
2.6	30	82.3	0.031	45.7	0.131	0.865
3	30	46.7	0.023	27.2	0.131	0.855
3.5	30	28.8	0.015	18.5	0.117	0.891
2.1	28	169.6	0.11	89.7	0.150	0.942
2.1	28	162.4	0.104	89.9	0.140	0.951
2.3	28	93.6	0.058	56.1	0.120	0.961
2.8	24	77.4	0.021	41.5	0.120	0.994
3.9	24	31.1	0.022	20.7	0.100	0.985
4.8	24	18.8	0.008	10.6	0.120	0.936
St-Alban						
3	1	27.3	0.023	24.2	0.054	0.750
3	2	39.5	0.029	34.5	0.053	0.817
3	4	49.6	0.031	41.1	0.060	0.910
3	10	59.7	0.032	51.4	0.050	0.908
3	30	67.3	0.032	53.3	0.065	0.866
Jonquière						
2	0.1	95.1	0.049	88.7	0.033	0.747
2	0.3	132.5	0.068	99.8	0.076	0.955

Table 2 (*continued*).

Group 1: low-activity soils						
		Bingham model		Normalized flow curve		
Liquidity index, I_L	Salinity, S (g/L)	Shear stress, τ_c (Pa)	Viscosity, η_h (Pa·s)	Reference shear stress, τ_o (Pa)	Power law index, n	Coefficient of determination, r^2
2	0.7	217.7	0.113	159.1	0.082	0.878
2	1.0	216.0	0.121	141.9	0.108	0.856
2	10.0	199.3	0.111	125.7	0.116	0.838
2	30.0	288.2	0.153	182.9	0.114	0.892
2.5	0.1	45.8	0.026	41.3	0.049	0.794
2.5	0.3	62.6	0.033	48.6	0.069	0.960
2.5	0.7	96.4	0.054	70.1	0.085	0.959
2.5	1.0	105.3	0.062	74.9	0.09	0.942
2.2	10.0	104.9	0.059	71.9	0.097	0.946
2.5	30.0	166.4	0.081	117.7	0.088	0.968
3	0.1	23.5	0.017	19.8	0.057	0.708
3	0.3	47.5	0.025	37.1	0.067	0.956
3	0.7	58.6	0.031	45.1	0.071	0.961
3	1.0	59.0	0.034	44.6	0.076	0.977
3.2	10.0	58.8	0.031	42.9	0.081	0.986
3.0	30.0	103.2	0.048	70.5	0.088	0.872
3.5	0.1	18.1	0.015	13.9	0.067	0.739
3.5	0.3	27.5	0.015	21.2	0.070	0.934
3.5	0.7	28.0	0.016	21.5	0.073	0.946
3.5	1.0	37.0	0.023	28.4	0.075	0.965
3.7	10.0	37.9	0.021	28.7	0.075	0.969
3.5	30.0	65.6	0.030	47.9	0.08	0.957
Group 2: high-activity Black sea soils						
		Bingham model		Normalized flow curve		
Liquidity index, I_L	Salinity, S (g/L)	Shear stress, τ_c (Pa)	Viscosity, η_h (Pa·s)	Reference shear stress, τ_o (Pa)	Power law index, n	Coefficient of determination, r^2
Black Sea 10						
2.1	23	128.7	0.260	59.7	0.209	0.936
2.8	23	111.8	0.214	59.3	0.170	0.972
3.0	23	35.2	0.066	20.3	0.162	0.929
3.8	23	13.2	0.035	7.3	0.194	0.927
Black Sea 20						
1.8	23	113.0	0.223	67.2	0.164	0.860
2.1	23	82.6	0.163	50.4	0.149	0.903
2.3	23	53.6	0.122	31.8	0.154	0.903
2.5	23	45.1	0.097	29.5	0.128	0.882
3.0	23	18.9	0.047	12.8	0.155	0.902
Group 2: high-activity bentonite soils						
		Bingham model		Normalized flow curve		
Liquidity index, I_L	Water content, w (%)	Shear stress, τ_c (Pa)	Viscosity, η_h (Pa·s)	Reference shear stress, τ_o (Pa)	Power law index, n	Coefficient of determination, r^2
Bentonite S = 0 g/L						
1.9	607.3	210.6	0.390	82.4	0.240	0.994
2.1	681.9	148.4	0.256	38.3	0.317	0.996
2.2	709.2	119.6	0.147	16.1	0.404	0.999
2.4	768.9	68.1	0.117	6.5	0.481	0.999
2.5	794.3	48.6	0.099	4.6	0.495	0.996

Table 2 (*concluded*).

Group 2: high-activity bentonite soils						
		Bingham model		Normalized flow curve		
Liquidity index, I_L	Water content, w (%)	Shear stress, τ_c (Pa)	Viscosity, η_h (Pa·s)	Reference shear stress, τ_o (Pa)	Power law index, n	Coefficient of determination, r^2
2.7	850.5	25.9	0.074	1.9	0.562	0.995
2.9	908.9	15.3	0.054	1.1	0.580	0.995
3.0	968.8	11.2	0.043	1.5	0.493	0.965
3.1	993.6	8.1	0.040	0.6	0.614	0.988
3.4	1033.5	7.1	0.035	1.1	0.499	0.960
Bentonite: S = 30 g/L						
1.7	201.6	303.6	0.414	217.8	0.100	0.973
1.8	219.6	238.2	0.248	158.9	0.113	0.948
1.9	228.9	194.6	0.199	131.8	0.109	0.941
2.0	235.1	192.1	0.160	115.1	0.130	0.965
2.1	244.5	174.4	0.092	93.3	0.139	0.948
2.2	249.8	130.9	0.076	69.3	0.144	0.943
2.3	254.2	126.2	0.076	67.5	0.144	0.941
2.6	279.7	77.1	0.050	40.4	0.151	0.944
2.6	286.4	62.5	0.044	32.9	0.152	0.934
2.9	306.2	44.1	0.033	22.9	0.158	0.933
3.2	340.0	22.7	0.022	11.7	0.172	0.920
Group 3: Silt-rich soils						
		Bingham model		Normalized flow curve		
Liquidity index, I_L	Water content, w (%)	Shear stress, τ_c (Pa)	Viscosity, η_h (Pa·s)	Reference shear stress, τ_o (Pa)	Power law index, n	Coefficient of determination, r^2
Iron tailings: flocculated						
1.5	25.8	55.2	1.131	17.6	0.479	0.968
1.9	28.4	81.9	0.346	15.3	0.434	0.990
2.4	31.3	62.9	0.252	20.3	0.328	0.982
2.6	32.4	23.7	0.076	9.7	0.297	0.916
4.2	42.3	9.8	0.037	4.7	0.285	0.874
Iron tailings: unflocculated						
2.1	26.2	89.5	1.129	21.6	0.649	0.978
2.2	26.9	87.6	1.095	25.1	0.439	0.927
2.3	27.2	70.9	1.190	7.3	0.430	0.945
2.5	27.9	56.0	0.471	8.2	0.549	0.992
2.8	27.3	56.9	0.521	3.4	0.581	0.993

Note: n is the power law index obtained from the normalized flow curve (eq. [4]).

CO viscometer for studying the <0.075 mm fraction of the French soils.

To examine the rheology of low-activity clays (group 1), natural muds and water in the container were thoroughly mixed using a blender to ensure complete homogenization for the given solid concentrations. Samples were then left to rest for 30 to 60 min to allow hydration and dispersion of the sediment particles. Salt content was measured as sodium chloride (NaCl) equivalent and was maintained constant during all tests for a given sample. The same test methods were used to investigate the rheology of silt-rich soils. As for the high-activity clays (group 2), bentonite powder was progressively dispersed in fresh or salt water (NaCl solution) and shaken for more than 10 min. All samples were mixed using a blender at high spin (approximately 3000 rpm) until mixtures were homogenous. They were then put in a jug and left for 24 h, allowing sufficient time to ensure uniform mixing and buildup of a gel-like structure before testing. All measurements were made at a room temperature of 21 to 22 °C. After testing, the liquidity index was slowly increased up to the next desired value while retaining constant salinity.

Rheological behaviour of low-activity clays

Most of the materials examined in this paper comprised clayey sediments reconstituted at a liquidity index between

2 and 4. Figure 1 presents shear stress – strain rate (τ–γ) relationships for the Jonquière clay, which had a clay fraction from 58% to 61%. All the tests were performed at the same salinity (1 g/L) but at different liquidity indices. Figure 1*a* shows the τ–γ relationships in a linear plot. It can be seen that the shear stress rapidly increases towards yield stress, but once it reaches this point, it increases more slowly. Referring to the Bingham model (eq. [1]), at a liquidity index of 2.0, τ_c would be equal to 216 Pa, and η_h would be equal to 0.121 Pa·s (see dashed line on Fig. 1*a*). It can be seen that the Bingham model well describes the rheological behaviour at strain rates larger than about 50 s^{-1}, but overestimates the shear stress at lower strain rates. It can also be seen that viscosity, η_h, decreases when the liquidity index increases.

Figure 1*b* presents the same results in a log(τ) versus log(γ) scale. From these graphs, it can be seen that: (*i*) the curves are essentially linear, indicating that the power law model applies for strain rates from 1 to 500 s^{-1}; (*ii*) the curves corresponding to liquidity indices between 2.0 and 3.5 are essentially parallel, which indicates that n is approximately constant for all the tests performed. The normalized flow curves according to eq. [4] are presented in Fig. 1*c*. The reference shear rate (γ_o) for normalization was taken to be equal to 1 s^{-1}. It can be seen that all the normalized flow curves lie close to a unique line with an average slope, n, equal to 0.09.

Figure 2 shows the flow curves obtained for the same Jonquière clay at a liquidity index of 2.0, but with salinities ranging from 0.1 to 30 g/L. Figure 2*a* presents the flow data in a linear plot, which is consistent with the Bingham model. It can be seen that both the yield stress τ_c and viscosity η_h of the Bingham law significantly increase with salinity. However, when the normalized flow curves are presented in a log–log scale corresponding to the power law model (Fig. 2*b*), they are essentially linear (which indicates that the power law applies), and are relatively close, having an average n value of 0.07. Similar behaviour was observed in St-Alban clay (Jeong et al. 2004). From Figs. 1 and 2, it appears that, for the Jonquière clay, the power law index, n, does not significantly vary with liquidity index and salinity. Figure 3 presents normalized flow curves obtained on other low-activity clays (e.g., the Adriatic Sea, Cambridge Fjord, Hudson Apron, Mediterranean Sea, Pointe-du-Fort, and St-Alban clays). It can be seen that the viscous behaviour is generally well represented by the power law for shear strain rates between 1 and 1000 s^{-1}, with average n values varying from 0.056 for St-Alban clay and 0.169 for Adriatic Sea sediments. The rheological parameters corresponding to the Bingham and power law models are given in Table 2. However, at very low shear rates between 1 and 3 s^{-1}, the power law deviates from the other data, particularly for the Adriatic Sea and Mediterranean Sea sediments (Figs. 3*a* and 3*d*); the power law applies globally to low-activity clays with power law indices n in the range of 0.06 to 0.17, with an average value of 0.12, which is similar to that of the Jonquière clay. This average n value corresponds to a change in shear stress of about 32% per logarithmic cycle of shear strain rate.

The power law (eq. [4]) is described by two parameters: the reference shear stress, τ_o, at the reference strain rate

Fig. 4. Relationship between liquidity index and reference shear stress in low-activity clays.

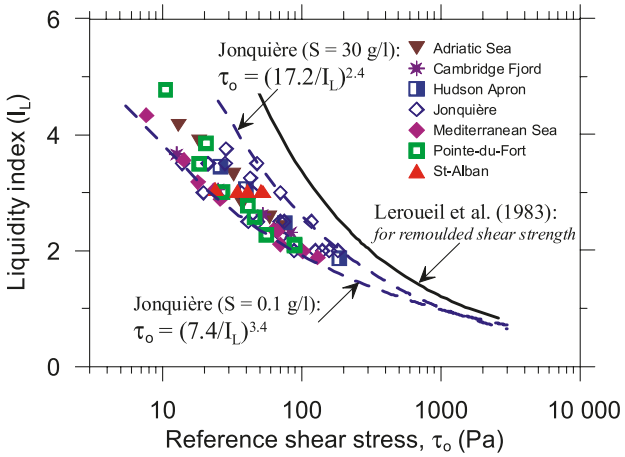

Fig. 5. Relationship between reference shear stress (τ_o) and Bingham yield stress (τ_c) in low-activity clays. Legend of symbols is the same as in Fig. 4.

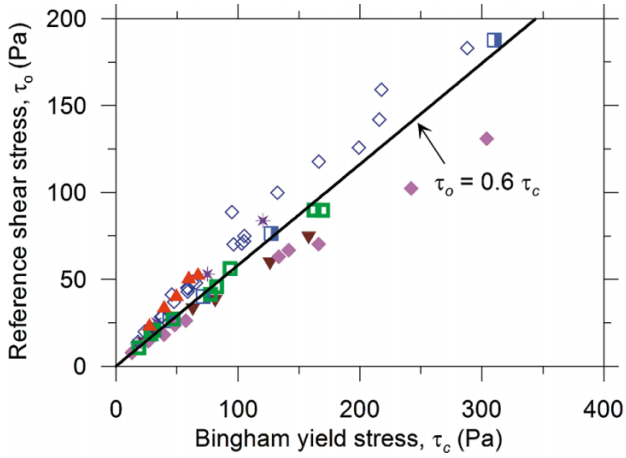

Fig. 6. Relationship between liquidity index, I_L, and normalized power law parameter, $n/n_{LI=3}$, in low-activity clays, where n is the power law parameter and $n_{LI=3}$ is the power law index defined at a liquidity index equal to 3.0.

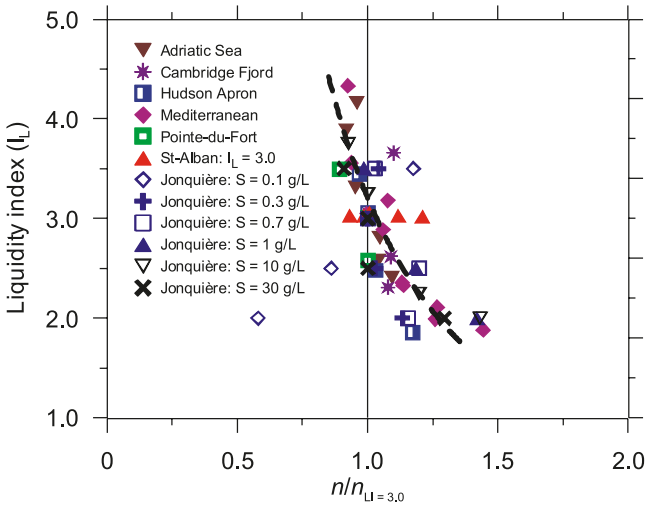

Fig. 7. Relationship between power law index, n, and plasticity index I_P as observed (*a*) in low-activity clayey soils and (*b*) in low-activity (group 1) and high-activity (group 2) clayey soils. Note that n_{mean} and $n_{LI = 3}$ are the mean n value and the n value at a liquidity index of 3.0, respectively.

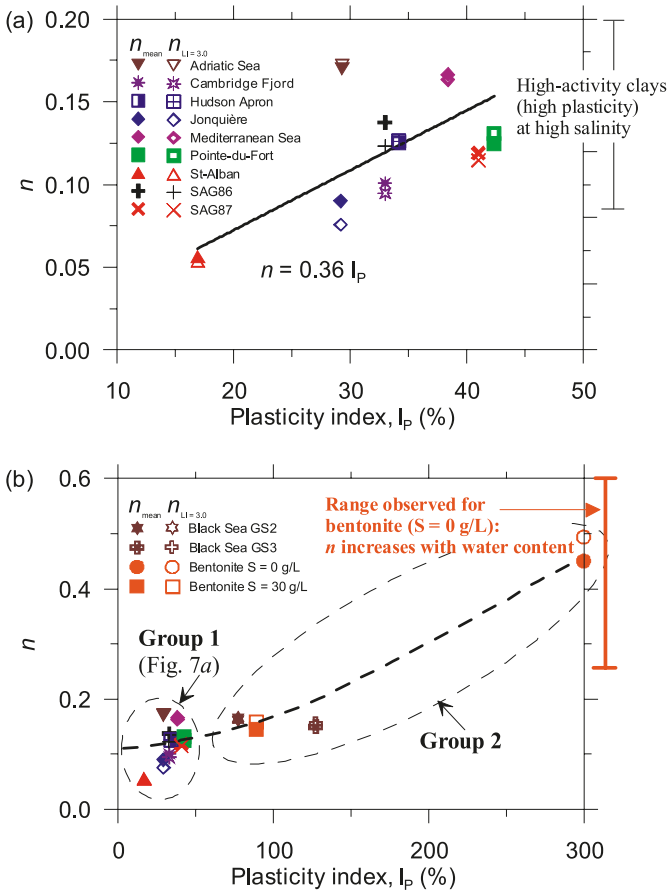

Fig. 8. Normalized flow curves of $\log(\tau / \tau_o)$ versus $\log(\gamma / \gamma_o)$ obtained on bentonite at different liquidity indices for salinities of (*a*) 30 and (*b*) 0 g/L.

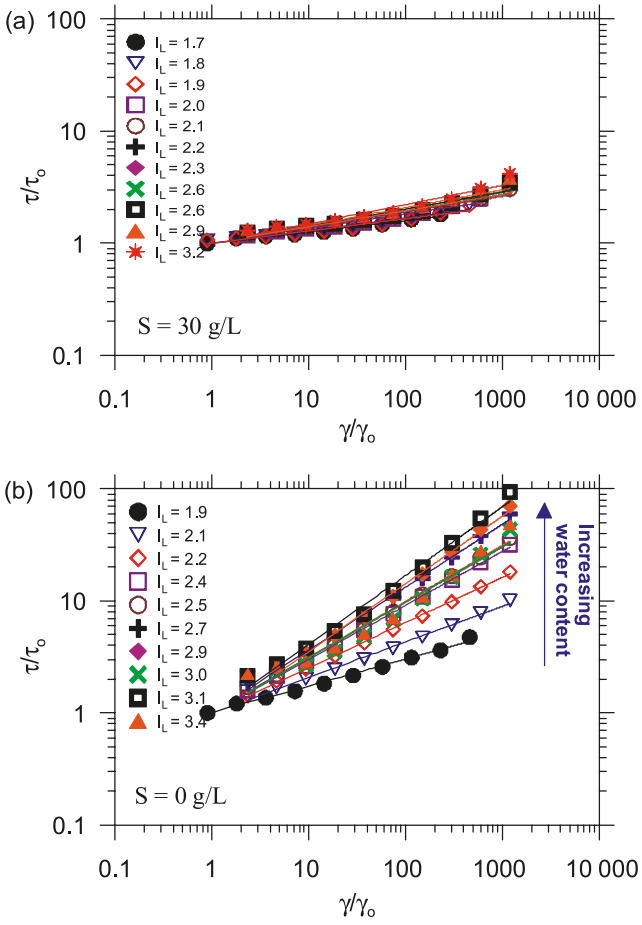

value, γ_o (taken here as equal to 1 s^{-1}), and the n value. The parameters τ_o and n are examined in this section. Figure 4 shows τ_o as a function of the liquidity index for the low-activity clays. The trend is similar to that observed for the remoulded shear strength (S_{ur}, in Pa) versus liquidity index presented by Leroueil et al. (1983) and also shown in Fig. 4. However, τ_o is 2 to 10 times smaller than the remoulded shear strength at the same liquidity index. The reference shear stress is also influenced by salinity. This is illustrated by the two dashed lines deduced from the tests performed on the Jonquière clay at salinities of 0.1 and 30 g/L. At the same liquidity index, τ_o increases with salinity. This is confirmed by the data obtained on St-Alban clay (Table 2). These results are generally consistent with those observed by Locat (1997) when he examined the yield stress (τ_c, in Pa) in the Bingham model as a function of the liquidity index. A comparison between the Bingham yield stress (τ_c), typically defined from test results in a range of shear strain rates between 100 and 500 s^{-1}, and τ_o value at a γ_o of 1 s^{-1} is shown in Fig. 5. The ratio of τ_o / τ_c is typically equal to 0.6 (r^2 = 0.96). This can also be seen on Figs. 1*a* and 2*a* where τ_c is clearly larger than the shear stress at a strain rate of 1 s^{-1}.

It has been indicated that n does not vary significantly with salinity and liquidity index. A detailed analysis of the n values presented in Table 2, however, shows that it does vary slightly with the liquidity index. To examine that point, $n/n_{LI = 3}$ ratios, where $n_{LI = 3}$ is the power law index defined at a liquidity index equal to 3.0, were plotted against liquidity indices for low-activity clays (Fig. 6). It can be seen that, with the exception of Jonquière clay (which is at a salinity of 0.1 g/L), all the results indicate a slight increase in n as liquidity index decreases, typically from 0.9 at a 4.5 liquidity index to 1.3 at a 2.0 liquidity index. Figure 7*a* shows the relationship between the power law index, n, and the plasticity index (I_P) for low-activity clays. Both the average n value and the n value at a liquidity index equal to 3.0 have been plotted on the figure. They are in fact very close. The figure shows some scatter, but indicates a tendency for the n value to increase with the plasticity index. An average relationship gives n = 0.36 I_P for low-activity clays when I_P is in the range of 15% to 45%.

Rheological behaviour of high-activity clays

Figure 8 shows the normalized flow curves obtained on bentonite at two different salinities (30 and 0 g/L) and different liquidity indices. They are essentially linear, indicating that the power law applies relatively well to these soils. At high salinity, n is approximately constant (Fig. 8*a*), with

Fig. 9. Reference shear stress, τ_o, and power law index, n, as functions of liquidity index in high-activity clays.

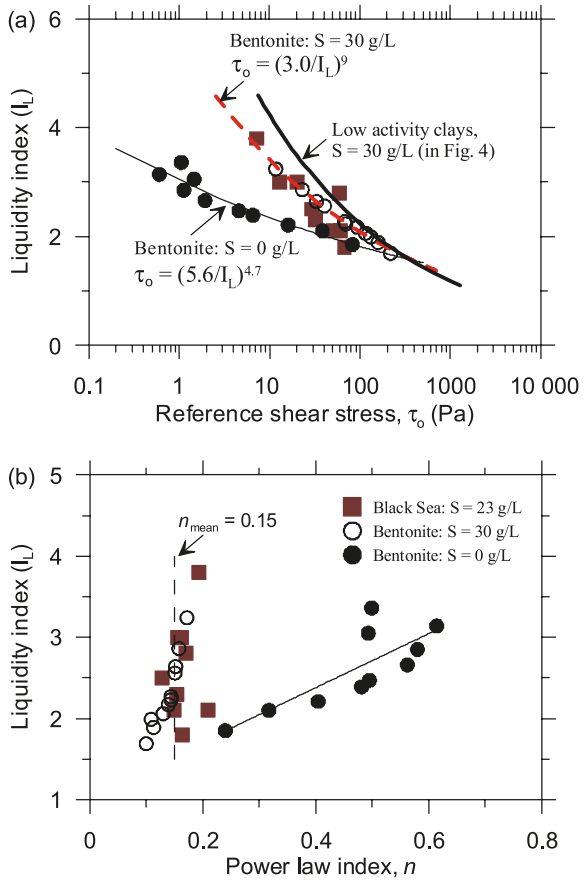

an average value of 0.14. At low salinity, however, n increases with water content (Fig. 8*b*), from 0.24 to 0.61 when the liquidity index increases from 1.9 to 3.4. Salinity thus plays an important role in the interaction between clay particles and pore water; this can be examined in terms of τ_o and n.

Figure 9 presents the reference shear stress, τ_o, and the power law index, n, as a function of liquidity index for the bentonite and the Black Sea clay. The τ_o–I_L relationships obtained on bentonite hydrated with salt water and the Black Sea clay (S = 23 g/L) are very similar, and just below that observed for low-activity clays at high salinity (Fig. 4). As for the n value, it is very similar for both the bentonite (S = 30 g/L) and the Black Sea clay and does not vary significantly with liquidity index at an average value of 0.15 (Fig. 9*b*). For bentonites at a salinity of 0 g/L and a given liquidity index, τ_o is much smaller than it is in the same soil at 30 g/L, and even smaller than it is in the Jonquière clay at low salinity (Fig. 9*a*), but n is much larger and increases with the liquidity index (Fig. 9*b*). Referring to Fig. 7*b*, which shows the power law index as a function of plasticity index for low- and high-activity clays, n seems to increase with the plasticity index.

The n values obtained from high-activity clays are plotted with those obtained from low-activity clays in Fig. 7*b*. The values obtained from bentonite and Black Sea mud at high salinity are close to those obtained from low-activity clays, indicating that n may not vary significantly for indices lower

Fig. 10. Normalized flow curves of $\log(\tau / \tau_o)$ versus $\log(\gamma / \gamma_o)$ obtained on iron tailings (*a*) when unflocculated and (*b*) when flocculated.

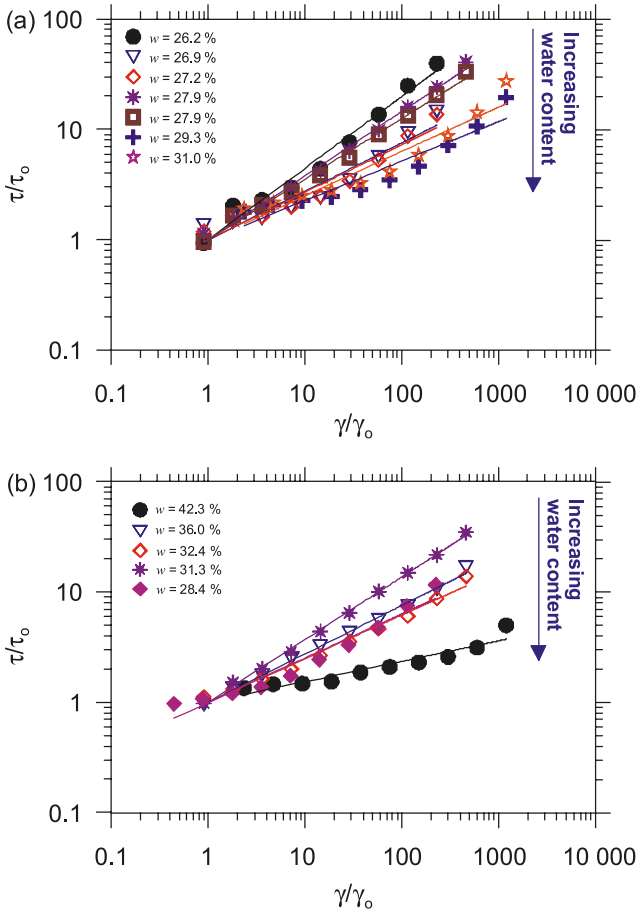

than 130% with an average value of about 0.14. This would be at variance with the conclusion deduced from Fig. 7*a*, but the number of test results is too limited to draw a definite conclusion. On the other hand, the bentonite (S of 0 g/L) that has a much higher plasticity index of 300% presents a higher n value, indicating that n could be influenced by plasticity. A curved relationship between n and I_p has been drawn on Fig. 7*b*.

Rheological behaviour of silt-rich soils

Figure 10 shows the normalized flow curves obtained at different water contents from iron tailings that were unflocculated (Fig. 10*a*) and flocculated (Fig. 10*b*). The experimental data are well represented by a linear log–log normalized flow curve (from eq. [4] when γ_o is taken as equal to 1 s^{-1}); thus, by power law, they are independent of the water content and soil fabric. However, the power law index, n, is very sensitive to small changes in water content, varying between 0.28 and 0.58. These values are much higher than the n values obtained in group 1 (n = 0.12 on average).

Malet et al. (2002, 2003) examined the rheological behaviour of silt-rich soils (i.e., those with soil fractions <0.075 mm) from the French Alps with the same coaxial (CO) viscometer. The test results are presented in Fig. 11 in

Fig. 11. Normalized flow curves of $\log(\tau / \tau_o)$ versus $\log(\gamma / \gamma_o)$ obtained on materials from the French Alps (data from Malet et al. 2003). Note that the geometry used was coaxial (CO). FAU, Faucon; POC, Poche; RBX, Riou-Bourdoux; VAL, La Valette.

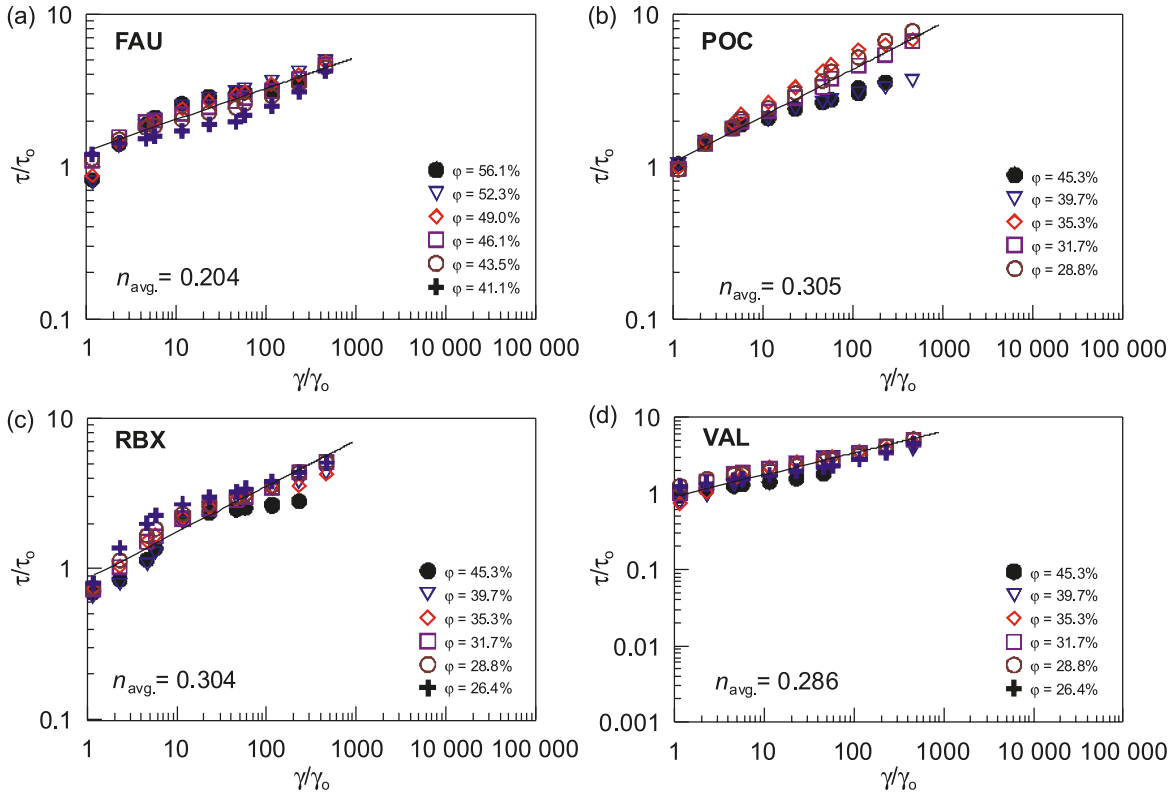

a normalized manner for different values of volumetric concentration of solid (φ, in %) and for shear strain rates between 1 and about 500 s^{-1}. In all cases, the reference shear rate γ_o is taken as equal to 1 s^{-1}. The curves can be approximated by linear log–log plots, as in low-activity clays. They result, however, in n values between 0.2 and 0.3, which are higher than those measured for both group 1 and the tailings.

Discussion

The results obtained in this study indicate that the power law applies to a large variety of remoulded soils, from high-activity clays to silts. For clays, the results are characterized by a reference shear stress τ_o that depends on the liquidity index and also on the salinity of pore water. They are also characterized by a power law index, n, that does not vary significantly with liquidity index, except for the bentonite at a salinity of 0 g/L. Apparently, n increases only slightly with increasing plasticity for I_p values lower than 130%, yielding typical values of 0.12 for low-activity clays and 0.15 for high-activity clays. However, it increases significantly with increasing plasticity at higher plasticity indices. For silt-rich soils, the power law index varies significantly with small changes in water content, and is found to be in the range of 0.2 to 0.6, which is higher than the power law indices of clays of low plasticity.

The power law describes well the rheological behaviour of soils over a range of strain rates between 1 and 1000 s^{-1}, i.e., in a range that is representative of strain rates in debris flows (0.1 to 20 s^{-1}). This is an advantage over the Bingham model that, practically, is representative of soil behaviour for shear strain rates larger than 50 s^{-1} and generally overestimates shear stresses at lower strain rates.

An n value of 0.12 for low-activity remoulded clays corresponds to a change in shear stress of 32% when the strain rate changes by one order of magnitude. It has been shown that the power law (eq. [4]) also applies well to intact low-activity clays with n values (which are equal to $C_{\alpha e}/C_c$ in one-dimensional compression) between 0.03 and 0.05, i.e., with a typical change in preconsolidation pressure or in undrained shear strength of 10% per log cycle of strain rate (Kulhawy and Mayne 1990; Mesri et al. 1995; Leroueil 1996, 2006). It would be interesting to try to understand why the power law index is so different in intact and remoulded clays. This is particularly true in sensitive clays, as the same material at the same water content may creep in under intact conditions and be involved in a mud flow. This was the case of a St-Jean-Vianney clay with a liquidity index >2 that was involved in a huge mud flow (Tavenas et al. 1971; Saihi et al. 2002). Obviously, intact and remoulded clays do not have the same fabric and microstructure and are not subjected to the same shear mode. However, there may also be an effect of strain rate at work.

Leroueil (2006) showed on the basis of laboratory oedometer tests and observations made under embankments built on several clayey sites that n is not perfectly constant, but increases with strain rate from about 0.02 ± 0.01 at a strain rate of 10^{-10} s^{-1} to about 0.06 ± 0.01 at a strain rate of 10^{-5} s^{-1}. This general trend is shown by a solid line on Fig. 12. Also

Fig. 12. Power law index, n, as a function of strain rate in low-activity clays. The arrow on the figure indicates the direction of increasing plasticity index of low-activity clays.

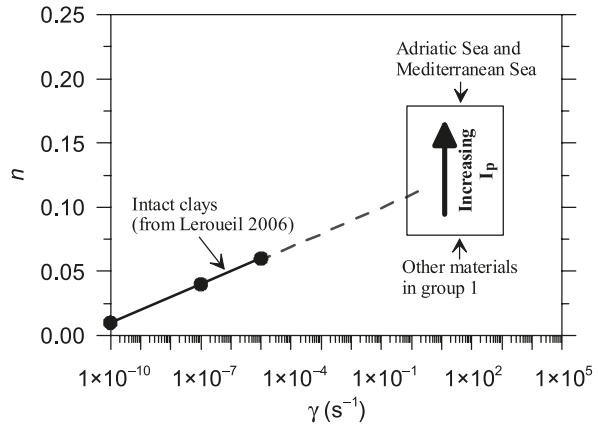

shown on this figure is the range of n values obtained in the viscometric tests performed on remoulded clays at the strain rates used in these tests. Two remarks can be made. First, the strain rates used in viscometric tests are much higher than those existing in conventional tests on intact clays (10^{-7} to 10^{-5} s^{-1}) or under embankments ($<10^{-7}$ s^{-1}). The second remark is that the n values deduced from viscometric tests appear to be in the continuity with those deduced from compression tests, indicating that n is possibly not constant but is strain-rate dependent. This would imply that the power law would not be valid for strain rates varying from 10^{-10} s^{-1} to 10^{3} s^{-1}, but could be applied only as a good approximation over a few orders of magnitude of strain rate.

Conclusion

The applicability of the power law for describing the rheological behaviour of soils has been presented. A data set was selected from recently reported experimental studies. The chosen representatives of groups are: (*i*) for low-activity clays, (*ii*) for high-activity clays, and (*iii*) for silt-rich soils. The main conclusions are deduced from tests in coaxial viscometer and are summarized as follows:

(1) The rheological behaviour of soils of different origins is relatively well described by the power law on a range of strain rates from about 1 to 1000 s^{-1}, thus it is representative of strain rates generally observed in debris flows (e.g., 0.5 to 20 s^{-1}). This is an advantage because the Bingham law model is generally not representative of the soil behaviour in that latter range of strain rates.

(2) The power law index, n, obtained from the normalized flow curve is examined for low-activity cohesive soils. It is essentially constant and is not very sensitive to changes in liquidity index and salinity. From the normalized flow curves examined for low-activity clays, the power law index, n, is typically equal to 0.12, corresponding to about a 32% variation in strength per logarithmic cycle of shear strain rate.

(3) For clayey soils in general, n seems to increase with the plasticity index. However, for high-activity clays (such as bentonite with S = 0 g/L), n is not constant, but increases with water content. Tests performed on silt-rich and coarser materials show that n is larger than for low-activity clays. The tests on silt-rich soils also show that n may vary significantly for small changes in water content.

(4) The power law appears to be valid over a few orders of magnitude of strain rate. However, it is possible that it could not apply over many orders of magnitude as the power law index, n, could be strain-rate dependent, increasing with strain rate.

Acknowledgements

The authors would like to thank the Natural Sciences and Engineering Research Council Canada who, via the COSTA-Canada Continental Slope Stability Project, provided the financial support. A special thanks to the anonymous reviewers for their valuable comments and corrections.

References

Coussot, P. 1997. Mudflow rheology and dynamics. IAHR Monograph Series. Balkema, Rotterdam, the Netherlands.

Imran, J., Harff, P., and Parker, G. 2001. A numerical model of submarine debris flows with graphical user interface. Computers & Geosciences, **27**(6): 717–729. doi:10.1016/S0098-3004(00)00124-2.

Iverson, R.M. 1997. The physics of debris flow. Reviews of Geophysics, **35**(3): 245–296. doi:10.1029/97RG00426.

Jeong, S.W. 2006. Influence of physico-chemical characteristics of fine-grained sediments on their rheological behavior. Ph.D. thesis, Department of Civil Engineering, Laval University, Québec City, Que.

Jeong, S.W., Locat, J., and Leroueil, S. 2004. A preliminary analysis of the rheological transformation due to water infiltration as a mechanism for high mobility of submarine mass movements. *In* Proceedings of the 57th Canadian Geotechnical Conference, Québec City, Que., 24–27 October 2004. BiTech Publishers Ltd., Richmond, B.C. Session 7G. pp. 15–22.

Kulhawy, F.H., and Mayne, P.W. 1990. Manual on estimating soil properties for foundation design.. Electric Power Research Institute, Palo Alto, Calif. Technical report EPRI-EL-6800

Leroueil, S. 1996. Compressibility of clays: fundamental and practical aspects. Journal of Geotechnical Engineering, **122**(7): 534–543. doi:10.1061/(ASCE)0733-9410(1996)122:7(534).

Leroueil, S. 2006. The Isotache Approach. Where are we 50 years after its development by Professor Šuklje? 2006 Prof. Šuklje's Memorial Lecture. *In* Proceedings of the XIII Danube-European Conference on Geotechnical Engineering, Ljubljana, Slovenia, 29–31 May 2006. Slovenian Geotechnical Society, Ljubljana, Slovenia. Vol. 1, pp. 55–88.

Leroueil, S., Tavenas, F., and Le Bihan, J.-P. 1983. Propriétés caractéristiques des argiles de l'est du Canada. Canadian Geotechnical Journal, **20**(4): 681–705. doi:10.1139/t83-076.

Locat, J. 1997. Normalized rheological behaviour of fine muds and their flow properties in a pseudoplastic regime. *In* Proceedings of the 1st International Conference on Debris-Flow Hazards Mitigation, San Francisco, Calif., 7–9 August 1997. *Edited by* C.L. Chen. American Society of Civil Engineers, New York. pp. 260–269.

Locat, J., and Demers, D. 1988. Viscosity, yield stress, remoulded strength, and liquidity index relationships for sensitive clays. Canadian Geotechnical Journal, **25**(4): 799–806. doi:10.1139/t88-088.

Lorenzini, G., and Mazza, N. 2004. Debris flow: Phenomenology and rheological modeling. WIT Press, Southampton, UK.

Major, J.J., and Pierson, T.C. 1992. Debris flow rheology: experimental analysis of fine-grained slurries. Water Resources Research, **28**(3): 841–857. doi:10.1029/91WR02834.

Malet, J.P., Remaître, A., Ancey, C., Locat, J., Meunier, M., and Maquaire, O. 2002. Caractérisation rhéologique des coulées de débris et des laves torrentielles du bassin marneux de Barcelonnette (Alpes-de-Haute-Provence, France). Premiers résultats. Rhéologie, **1**: 17–25.

Malet, J.P., Remaître, A., Maquaire, O., Ancey, C., and Locat, J. 2003. Flow susceptibility of heterogeneous marly formations. Implications for torrent hazard control in the Barcelonnette basin (Alpes-de-Haute-Provence, France). *In* Proceedings of the 3rd International Conference on Debris-Flow Hazards Mitigation, 10–12 September 2003, Davos, Switzerland. *Edited by* D. Rickenmann and C.L. Chen. Millpress, Rotterdam, the Netherlands. pp. 351–362.

Mesri, G., Shahien, M., and Feng, T.W. 1995. Compressibility parameters during primary consolidation. *In* Proceedings of the International Symposium on Compression and Consolidation of Clayey Soils – IS-Hiroshima '95, Hiroshima, Japan, 10–12 May 1995. A.A. Balkema, Rotterdam, the Netherlands. Vol. 2. pp. 1021–1037.

O'Brien, J.S., and Julien, P.Y. 1988. Laboratory analysis of mud flow properties. Journal of Hydraulic Engineering, **114**(8): 877–887. doi:10.1061/(ASCE)0733-9429(1988)114:8(877).

Ochiai, H., Okada, Y., Furuya, G., Okura, Y., Matsui, T., Sammori, T., Terajima, T., and Sassa, K. 2004. A fluidized landslide on a natural slope by artificial rainfall. Landslides, **1**(3): 211–219. doi:10.1007/s10346-004-0030-4.

Parsons, J., Whipple, K., and Simoni, A. 2001. Experimental study of the grain flow, fluid-mud transition in debris flow. The Journal of Geology, **109**(4): 427–447. doi:10.1086/320798.

Perret, D., Locat, J., and Martignoni, P. 1996. Thixotropic behavior during shear of a fine-grained mud from Eastern Canada. Engineering Geology, **43**(1): 31–44. doi:10.1016/0013-7952(96)00031-2.

Phillips, C.J., and Davies, T.R.H. 1991. Determining rheological parameters of debris flow material. Geomorphology, **4**(2): 101–110. doi:10.1016/0169-555X(91)90022-3.

Saihi, F., Leroueil, S., La Rochelle, P., and French, I. 2002. Behaviour of the stiff and sensitive Saint-Jean-Vianney clay in intact, destructured and remoulded conditions. Canadian Geotechnical Journal, **39**(5): 1075–1087. doi:10.1139/t02-053.

Takahashi, T. 1981. Debris flow. Annual Review of Fluid Mechanics, **13**(1): 57–77. doi:10.1146/annurev.fl.13.010181.000421.

Tavenas, F., Chagnon, J.-Y., and La Rochelle, P. 1971. The Saint-Jean-Vianney landslide: observations and eyewitnesses accounts. Canadian Geotechnical Journal, **8**(3): 463–478. doi:10.1139/t71-048.